Vol 18 No 10, October 2009
1674-1056/2009/18(10)/4407–06

Chinese Physics B

© 2009 Chin. Phys. Soc.
and IOP Publishing Ltd

Phase-field simulation of the effect of interaction among ordered domains on interdiffusion in Ni–Al–Cr alloys*

Zhang Yu-Xiang(张玉祥), Wang Jin-Cheng(王锦程)†,
Yang Yu-Juan(杨玉娟), Yang Gen-Cang(杨根仓), and Zhou Yao-He(周尧和)

State Key Laboratory of Solidification Processing, Northwestern Polytechnical University, Xi'an 710072, *China*

(Received 8 January 2009; revised manuscript received 9 April 2009)

The effect of interaction among γ' ordered domains on the interdiffusion process in $\gamma+\gamma'/\gamma$ and $\gamma+\gamma'/\gamma+\gamma'$ diffusion couples is investigated by using the phase-field method, in which bulk free energy and mobility are linked with thermodynamic and kinetic databases. Simulated results show that the interaction among γ' ordered domains has great influence on the microstructure, the interdiffusion velocity and the volume fraction of γ' phase on both sides of the diffusion couples.

Keywords: interdiffusion, phase-field method, ordered domain, Ni–Al–Cr
PACC: 6630N, 8130H, 6470K

1. Introduction

Diffusion couples are formed by joining two different alloys together so that they are intimately contacted between two faces. Interdiffusion is the process where atoms diffuse from one side of a diffusion couple to the other side. Interdiffusion is of great importance in many subjects of materials science, including electrical contacts, thin film devices, high-temperature coatings and composite materials.

Due to the importance of interdiffusion, many researchers have paid much attention to the interdiffusion study. Morral *et al*[1−6] and Dayananda *et al*[7−11] concentrated on one-dimensional diffusion process from the analytical perspective. In the numerical simulation aspect, most studies are also limited to one dimension and fail to take morphologies of various phases into account. The phase-field method, a powerful tool in microstructure simulation, has been used to investigate the interdiffusion process. Among these various methods for the interdiffusion prediction, the phase-field method can be used to predict microstructure morphology and phase constitution with a remarkable accuracy.[12] Using the phase-field method, Wu *et al*[13,14] studied the interdiffusion process of prototype alloys, especially the microstructure evolution in interdiffusion zone, the movement of Kirkendall markers and the Type 0 boundary of two-phase diffusion couples. Recently, they also predicted the interdiffusion microstructures of the $\beta+\gamma/\gamma$ and $\beta+\gamma/\beta+\gamma$ diffusion couples in Ni–Al–Cr alloys.[15] In their work, it is claimed that the antiphase relation among ordered phase particles has no effect on the interdiffusion process. However, it is universally received that the interdiffusion process is affected by the microstructures when the volume fraction of second phase is high.[13,16] Wang *et al*[17,18] concluded that the ordered nature of the precipitates could affect the morphology of the mesoscopic microstructure in diffusion-controlled growth process. Thus, it is expected that the ordered domains can also affect the morphology in both halves of diffusion couples, so it is also expected that this interaction will influence the interdiffusion process.

In the present study, the phase-field method is used to investigate the effect of antiphase relation of γ' ordered phase on the interdiffusion process of the $\gamma+\gamma'/\gamma$ and $\gamma+\gamma'/\gamma+\gamma'$ diffusion couples in the Ni–Al–Cr alloys. The bulk free energy and the mobility are linked with the available databases by the calculation of phase diagrams (CALPHAD) method.

*Project supported by the National Natural Science Foundation of China (Grant No 50401013) and the National Defense Pre-research Foundation of China (Grant No 9140A12020108HK0333).
†Corresponding author. E-mail: jchwang@nwpu.edu.cn

2. Model

2.1. Gibbs free energy

In an Ni–Al–Cr ternary alloy system, the γ' precipitate possesses an ordered $L1_2$ structure and can be described by using a compound energy model with four sublattices: (Al, Cr, Ni)$_{0.25}$(Al, Cr, Ni)$_{0.25}$(Al, Cr, Ni)$_{0.25}$(Al, Cr, Ni)$_{0.25}$. $y^1_{\rm Al}$, $y^2_{\rm Al}$, $y^3_{\rm Al}$ and $y^4_{\rm Al}$ are used to denote the site fractions of Al at sites of 1, 2, 3 and 4, respectively. Similarly, $y^1_{\rm Cr}$, $y^2_{\rm Cr}$, $y^3_{\rm Cr}$ and $y^4_{\rm Cr}$ denote the site fractions of Cr at sites of 1, 2, 3 and 4, respectively. The relationship among the site fraction, composition and long-range order parameters can be written as

$$\begin{aligned}
y^1_{\rm Al} &= c_{\rm Al}\left(1-\eta_1-\eta_2+\eta_3\right),\\
y^2_{\rm Al} &= c_{\rm Al}\left(1-\eta_1+\eta_2-\eta_3\right),\\
y^3_{\rm Al} &= c_{\rm Al}\left(1+\eta_1-\eta_2-\eta_3\right),\\
y^4_{\rm Al} &= c_{\rm Al}\left(1+\eta_1+\eta_2+\eta_3\right),\\
y^1_{\rm Cr} &= c_{\rm Cr}\left(1-\eta'_1-\eta'_2+\eta'_3\right),\\
y^2_{\rm Cr} &= c_{\rm Cr}\left(1-\eta'_1+\eta'_2-\eta'_3\right),\\
y^3_{\rm Cr} &= c_{\rm Cr}\left(1+\eta'_1-\eta'_2-\eta'_3\right),\\
y^4_{\rm Cr} &= c_{\rm Cr}\left(1+\eta'_1+\eta'_2+\eta'_3\right),
\end{aligned} \tag{1}$$

where $c_{\rm Al}$ and $c_{\rm Cr}$ are the molar fractions of Al and Cr, η_i and η'_i $(i=1,2,3)$ are the corresponding long-range parameters. The relationship among Ni, Al and Cr site fractions can be expressed as $y^s_{\rm Ni}+y^s_{\rm Al}+y^s_{\rm Cr}=1$ $(s=1,2,3,4)$. The composition of Al and Cr can be related by the site fraction as

$$\begin{aligned}
c_{\rm Al} &= \frac{1}{4}\left(y^1_{\rm Al}+y^2_{\rm Al}+y^3_{\rm Al}+y^4_{\rm Al}\right),\\
c_{\rm Cr} &= \frac{1}{4}\left(y^1_{\rm Cr}+y^2_{\rm Cr}+y^3_{\rm Cr}+y^4_{\rm Cr}\right).
\end{aligned} \tag{2}$$

The molar Gibbs free energy of γ' ordered phase in the Ni–Al–Cr ternary alloy system can be written by using a four-sublattice model as follows:

$$\begin{aligned}
&G_m^{\rm order}\\
&=\sum_{i=\rm Al}^{\rm Ni} c_i\,{}^0G_i^{\rm fcc}+\sum_{i=\rm Al}^{\rm Ni}\sum_{j=\rm Al}^{\rm Ni}\sum_{k=\rm Al}^{\rm Ni}\sum_{l=\rm Al}^{\rm Ni} y_i^1y_j^2y_k^3y_l^4\,\Delta^0G^{\rm L1_2}_{ijkl}\\
&\quad+\sum_{\rm s=1}^{4}\left(\frac{RT}{4}\sum_{i=\rm Al}^{\rm Ni} y_i^s\ln\left(y_i^s\right)\right)+\Delta^{xs}G_m^{\rm L1_2},
\end{aligned} \tag{3}$$

in which ${}^0G^{\rm fcc}_{\rm Al}$, ${}^0G^{\rm fcc}_{\rm Cr}$ and ${}^0G^{\rm fcc}_{\rm Ni}$ are the Gibbs energy of pure Al, Cr and Ni in the non-magnetic fcc state, $\Delta^{xs}G_m^{\rm L1_2}$ is the excess energy of mixing, and $\Delta^0G^{\rm L1_2}_{ijkl}$ is the Gibbs free energy for the formation of the $ijkl$-type compound with i,j,k,l atom in 1, 2, 3, 4 sites, respectively.

The Gibbs free energies of γ and γ' phases in the ternary Ni–Al–Cr system can be described by a single function as a sum of the Gibbs free energy of disordered phase and the ordering energy,[19,20]

$$\begin{aligned}
&G\left(c_{\rm Al},c_{\rm Cr},\eta_i,\eta'_i\right)\\
&=G^{\rm dis}\left(c_{\rm Al},c_{\rm Cr}\right)+\Delta G^{\rm order}\left(c_{\rm Al},c_{\rm Cr},\eta_i,\eta'_i\right),
\end{aligned} \tag{4}$$

where $G^{\rm dis}\left(c_{\rm Al},c_{\rm Cr}\right)$ is the Gibbs free energy of the disordered phase, $i=1,2,3$. Also, the ordering energy $\Delta G^{\rm order}\left(c_{\rm Al},c_{\rm Cr},\eta_i,\eta'_i\right)$ is expressed as

$$\begin{aligned}
&\Delta G^{\rm order}\left(c_{\rm Al},c_{\rm Cr},\eta_i,\eta'_i\right)\\
&=G^{\rm order}\left(c_{\rm Al},c_{\rm Cr},\eta_i,\eta'_i\right)\\
&\quad-G^{\rm order}\left(c_{\rm Al},c_{\rm Cr},\eta_i=\eta'_i=0\right).
\end{aligned} \tag{5}$$

The bulk free energy in the Ni–Al–Cr system described by the CALPHAD method can be directly used in the phase-field model.

2.2. Phase-field model

The total free energy in the phase-field model is given by the sum of the bulk free energy and the gradient energy as

$$\begin{aligned}
F=\int_V\Bigg[&f\left(c_{\rm Al},c_{\rm Cr},\eta_i,\eta'_i\right)+\sum_{i,j=\rm Al,Cr}\left(\alpha_{ij}\nabla c_i\nabla c_j\right)\\
&+\sum_{i=1}^{3}\frac{\beta}{2}\left(\nabla\eta_i\right)^2+\sum_{i=1}^{3}\frac{\beta'}{2}\left(\nabla\eta'_i\right)^2\Bigg]{\rm d}V,
\end{aligned} \tag{6}$$

where $f\left(c_{\rm Al},c_{\rm Cr},\eta_i,\eta'_i\right)=G\left(c_{\rm Al},c_{\rm Cr},\eta_i,\eta'_i\right)/V_m$, V_m is the molar volume, α_{ij}, β and β' are the gradient energy coefficients. Microstructure evolution is described by solving the Cahn–Hilliard nonlinear diffusion equation and the Ginzburg–Landau equations,[20]

$$\begin{aligned}
\frac{\partial c_i}{\partial t}&=\sum_j\nabla\cdot\left(\tilde{M}_{ij}\nabla\frac{\delta F}{\delta c_j}\right),\quad i,j=\rm Al,Cr,\\
\frac{\partial\eta_i}{\partial t}&=-L_{ii}\frac{\delta F}{\delta\eta_i},\quad i=1,2,3,\\
\frac{\partial\eta'_i}{\partial t}&=-L'_{ii}\frac{\delta F}{\delta\eta'_i},\quad i=1,2,3,
\end{aligned} \tag{7}$$

where L_{ii} and L'_{ii} are the kinetic coefficients to characterise structure relaxation. $\tilde{M}_{ij}$ $(i,j=\rm Al,Cr)$ are the chemical mobilities defined in the laboratory reference system, which can be related to the atomic mobilities of $M_{\rm Al}$, $M_{\rm Cr}$ and $M_{\rm Ni}$ by Eq.(8),

$$\tilde{M}_{\mathrm{CrCr}} = V_m \left[c_{\mathrm{Cr}} \left(1 - c_{\mathrm{Cr}}\right)^2 M_{\mathrm{Cr}} + c_{\mathrm{Cr}}^2 c_{\mathrm{Al}} M_{\mathrm{Al}} + c_{\mathrm{Cr}}^2 c_{\mathrm{Ni}} M_{\mathrm{Ni}} \right],$$
$$\tilde{M}_{\mathrm{CrAl}} = V_m \left[-c_{\mathrm{Cr}} c_{\mathrm{Al}} \left(1 - c_{\mathrm{Cr}}\right) M_{\mathrm{Cr}} - \left(1 - c_{\mathrm{Al}}\right) c_{\mathrm{Cr}} c_{\mathrm{Al}} M_{\mathrm{Al}} + c_{\mathrm{Cr}} c_{\mathrm{Al}} c_{\mathrm{Ni}} M_{\mathrm{Ni}} \right],$$
$$\tilde{M}_{\mathrm{AlAl}} = V_m \left[c_{\mathrm{Al}}^2 c_{\mathrm{Cr}} M_{\mathrm{Cr}} + c_{\mathrm{Al}} \left(1 - c_{\mathrm{Al}}\right)^2 M_{\mathrm{Al}} + c_{\mathrm{Al}}^2 c_{\mathrm{Ni}} M_{\mathrm{Ni}} \right], \quad (8)$$

where the atomic mobilities of M_{Al}, M_{Cr} and M_{Ni} for Al, Cr and Ni are expressed as,[21]

$$M_i = \frac{1}{RT} \exp\left(\frac{-\Delta Q_i^*}{RT}\right) \quad (i = \mathrm{Al}, \mathrm{Cr}, \mathrm{Ni}), \quad (9)$$

where R is the gas constant, T temperature and ΔQ_i^* the diffusional activation energy.

3. Results and discussion

In this study, the temperature is 1373 K, the gradient energy coefficients take the values of $\alpha_{\mathrm{AlAl}} = \alpha_{\mathrm{CrCr}} = \alpha_{\mathrm{CrAl}} = 2.5 \times 10^{-9}$ J/m and $\beta = \beta' = 7.3 \times 10^{-12}$ J/m.[19] The dimensionless time step and spatial step are 0.0005 and 1.0, respectively. The dimensionless kinetic coefficients are $\widehat{L}_{ii} = \widehat{L'}_{ii} = 1.0$. The control equations are solved by the semi-implicit Fourier spectral method.[22,23]

Two groups of diffusion couples, $\gamma + \gamma'/\gamma$ and $\gamma + \gamma'/\gamma + \gamma'$, are investigated. For each group, two diffusion couples are studied: one has one kind of ordered domain and the other has four kinds of ordered domains on the left side. Because we only focus on the effect of antiphase relation of ordered domains on the interdiffusion processes, the elastic field is not taken into account in the present study.

3.1. $\gamma + \gamma'/\gamma$ diffusion couple

Two different sets of diffusion couples with one or four types of ordered domains on the left side are studied. The initial average composition of Al and Cr is $\bar{c}_{\mathrm{Al}}^{\mathrm{L}} = 0.16$ and $\bar{c}_{\mathrm{Cr}}^{\mathrm{L}} = 0.07$ on the left side and $\bar{c}_{\mathrm{Al}}^{\mathrm{R}} = 0.16$ and $\bar{c}_{\mathrm{Cr}}^{\mathrm{R}} = 0.07$ on the right side. Initially, the γ' precipitates on both sides randomly distribute in the disordered matrix following the Gaussian distribution. The same seeds are used in all the diffusion couples to assure that the distribution is identical.

Figure 1 shows the microstructural evolution of the diffusion couple with one type of ordered domain on the left side (the gray levels represent the composition of Al). It can be seen that the microstructure coarsens severely and the γ' precipitates coalesce to form larger particles. As shown in Figs.1(b) and 1(c), the γ' particles with irregular shapes are found in the left half of the diffusion couple.

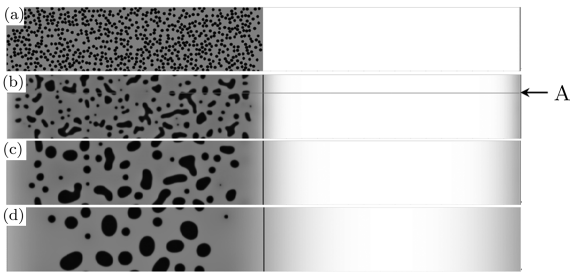


Fig.1. Morphology evolutions in $\gamma + \gamma'/\gamma$ diffusion couple (with one kind of domains) with initial average composition of $\bar{c}_{\mathrm{Al}}^{\mathrm{L}} = 0.16$, $\bar{c}_{\mathrm{Cr}}^{\mathrm{L}} = 0.07$, $\bar{c}_{\mathrm{Al}}^{\mathrm{R}} = 0.1$, and $\bar{c}_{\mathrm{Cr}}^{\mathrm{R}} = 0.08$ at different times: $t = 0$ (a), 10000 (b), 40000 (c) and 140000 (d).

Figure 2 shows the microstructure evolution in the diffusion couple with four types of ordered domains. Analogously, it is also found that the γ' particles coarsen significantly. However, from Figs.1 and 2, it is shown that the microstructures are obviously different in the two diffusion couples. For example, at $t = 10000$, the particles in Fig.1 are more irregular than those in Fig.2. The particles in Fig.2 keep separated while those in Fig.1 interconnected, which results from the different interactions among the ordered domains.

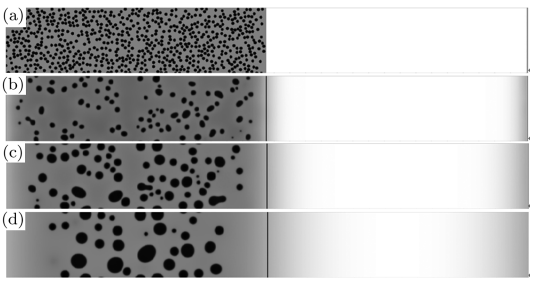


Fig.2. Morphology evolutions in $\gamma + \gamma'/\gamma$ diffusion couple (with four types of domains) with the initial average composition of $\bar{c}_{\mathrm{Al}}^{\mathrm{L}} = 0.16$, $\bar{c}_{\mathrm{Cr}}^{\mathrm{L}} = 0.07$, $\bar{c}_{\mathrm{Al}}^{\mathrm{R}} = 0.1$, $\bar{c}_{\mathrm{Cr}}^{\mathrm{R}} = 0.08$ at different times: $t = 0$ (a), 10000 (b), 40000 (c) and 140000 (d).

In the precipitate growth and the coarsening processes, two mechanisms appear: the conventional

Ostwald ripening and the coalescence of neighboring particles.[18] In the conventional Ostwald ripening process, the atoms transfer from one particle to another through the matrix. The particles smaller in size disappear while those of a bigger size grow. However, in the mechanism of coalescence, neighbouring particles coalesce into larger ones. In the four-domain system, there are four types of γ' ordered particles, so there are two relations: "in-phase" and "out-of-phase" between any two particles. Furthermore, the chance for each of them to appear is nearly identical, so the chance for the neighbouring particles to be "in-phase" (the same type of particles) is 25%.[18] However, in the system with only one type of ordered domain, all particles are "in-phase". So it is obvious that the coalescence of neighbouring particles in the one-domain system is more frequent than in the four-domain system. The different interactions between particles lead to the difference between the above mechanisms on the diffusion couple. In the one-domain system, the coalescence mechanism of neighbouring particles occurs more frequently than in the four-domain system.

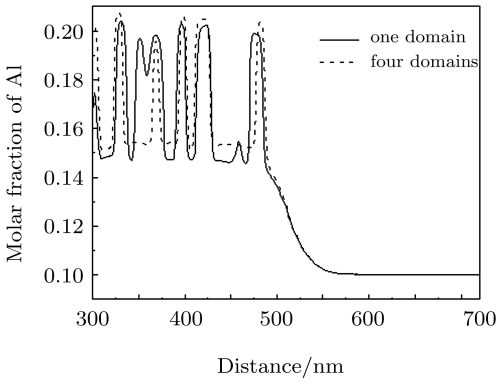


Fig.3. Composition profiles along the arrow shown in Fig.1(b) at $t = 10000$ for the two diffusion couples.

In the Ni–Al–Cr alloy system, when the γ' particles dissolve in the Ostwald ripening process, the composition of Al in the matrix increases. Figure 3 shows the composition profiles of Al along the line shown by an arrow 'A' at $t = 10000$ for the two diffusion couples. It is found that in the left half, the Al composition in the matrix of the four-domain system is higher than that in the one-domain system, while the compositions of Al are nearly the same in the right half of these two diffusion couples. Consequently, the gradients of Al composition are different in these two diffusion couples: the gradient of Al composition in the four-domain system is larger than that in the one-domain system near the initial coupling interface.

Figure 4 shows the volume fractions of the γ' precipitate as a function of time for these two diffusion couples (the symbols are obtained by the phase-field method and the lines are the corresponding B-spline fitting results). A decrease of the volume fraction of γ' precipitate is found in the left half of the two diffusion couples. Moreover, the curve of the volume fraction for the four-domain system is lower than that for the one-domain system, which indicates that Al atoms in the four-domain system diffuse faster than that in the one-domain system.

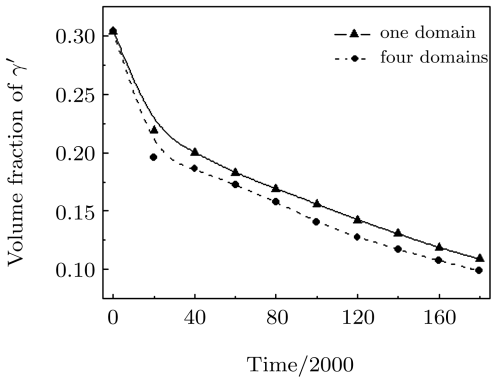


Fig.4. Volume fractions of γ' phase on the left side of diffusion couples as a function of time.

3.2. $\gamma + \gamma'/\gamma + \gamma'$ diffusion couple

To further assure the effect of antiphase relation on interdiffusion process, the $\gamma + \gamma'/\gamma + \gamma'$ diffusion couples are also investigated to confirm the regularity found in the $\gamma + \gamma'/\gamma$ diffusion couples.

Similarly, two diffusion couples are studied: one with one type of ordered domain and the other with four types of ordered domains in the left half. In the right half, there are four types of ordered domains for both diffusion couples. Distributions of γ' precipitates are identical in these two diffusion couples. For all $\gamma + \gamma'/\gamma + \gamma'$ diffusion couples, the initial average composition of Al and Cr is $\bar{c}^{\mathrm{L}}_{\mathrm{Al}} = 0.16$, $\bar{c}^{\mathrm{L}}_{\mathrm{Cr}} = 0.07$ on the left side and $\bar{c}^{\mathrm{R}}_{\mathrm{Al}} = 0.17$, $\bar{c}^{\mathrm{R}}_{\mathrm{Cr}} = 0.1$ on the right side.

Due to the same reason as in $\gamma + \gamma'/\gamma$ diffusion couples, on the left side of the one-domain system, the neighbouring γ' precipitates interconnect with each other and the corresponding γ' particles are irregular (see Fig.5). However, as shown in Fig.6, in the four-domain system the shape of the γ' precipitates

in the left half of the diffusion couple is more regular than in the one-domain system, and the regularity is the same as in the $\gamma + \gamma'/\gamma$ diffusion couples.

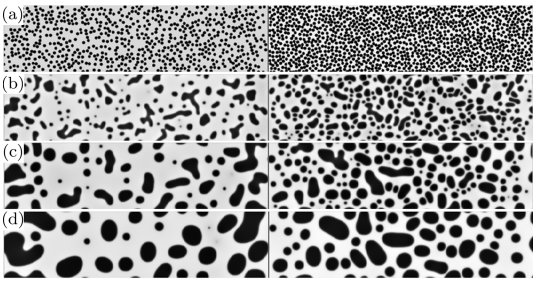


Fig.5. Morphology evolutions in $\gamma + \gamma'/\gamma + \gamma'$ diffusion couple (with one kind of domains) with initial average composition of $\bar{c}^{\mathrm{L}}_{\mathrm{Al}} = 0.16$, $\bar{c}^{\mathrm{L}}_{\mathrm{Cr}} = 0.07$, $\bar{c}^{\mathrm{R}}_{\mathrm{Al}} = 0.17$, $\bar{c}^{\mathrm{R}}_{\mathrm{Cr}} = 0.1$ at different times: $t = 0$ (a), 10000 (b), 40000 (c) and 140000 (d).

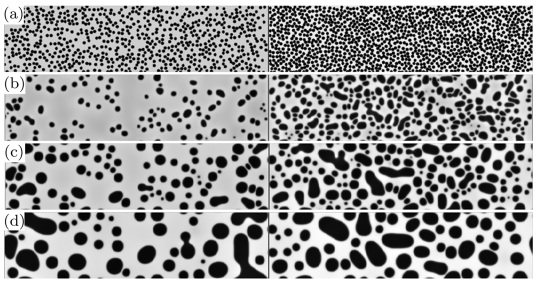


Fig.6. Morphology evolutions in $\gamma + \gamma'/\gamma + \gamma'$ diffusion couple (with four domains) with initial average composition of $\bar{c}^{\mathrm{L}}_{\mathrm{Al}} = 0.16$, $\bar{c}^{\mathrm{L}}_{\mathrm{Cr}} = 0.07$, $\bar{c}^{\mathrm{R}}_{\mathrm{Al}} = 0.17$, $\bar{c}^{\mathrm{R}}_{\mathrm{Cr}} = 0.1$ at different times: $t = 0$ (a), 10000 (b), 40000 (c) and 140000 (d).

Figure 7 shows the composition profiles of Al along the diffusion direction (at the same position shown by the arrow 'A' in Fig.1(b)) at $t = 10000$ for the two diffusion couples. During the early stage of coarsening process, the γ' particle smaller in size dissolves in the matrix, leading to the increase of Al composition in the matrix. In the left half of the diffusion couple, the Al composition in the matrix of the four-domain system is higher than that of the one-domain system. In the right half of these two diffusion couples, due to the same antiphase relation and the same distribution of γ' particles, the Al compositions in the matrix are close to each other. In the matrix of the four-domain system, the Al composition increases. So the gradient of Al in the four-domain system is smaller than that in the one-domain system near the initial coupling interface region.

Figure 8 shows the volume fractions of γ' phase on the left and the right sides of diffusion couples as a function of time (the lines are the corresponding B-spline fitting results). It is seen that Al diffuses along its own composition gradient (from the right to the left of the diffusion couple), as a result, the volume fraction of the γ' precipitate decreases in the right half while increasing in the left half. In the left half of the diffusion couple, the volume fraction of the γ' precipitate in the four-domain system is lower than that in the one-domain system. Correspondingly, in the right half, the volume fraction of the γ' precipitate in the four-domain system is greater than that in the one-domain system.

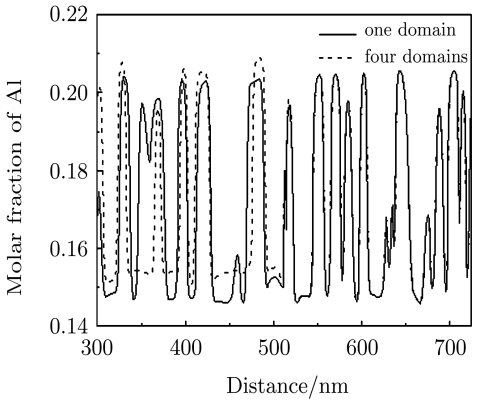


Fig.7. Composition profiles for Figs.5(b) and 6(b) at $t = 10000$ for the two diffusion couples.

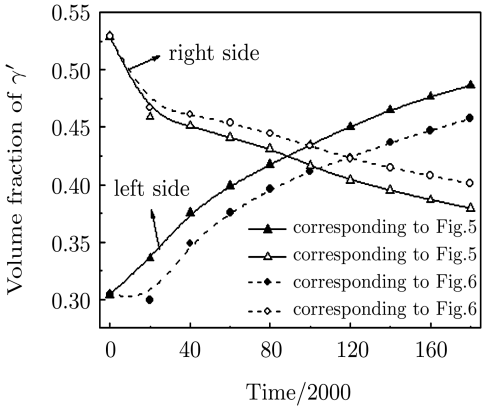


Fig.8. Volume fractions of γ' phase of the left and the right sides of diffusion couples as a function of time.

4. Conclusion

In conclusion of this paper, by linking the bulk free energy and mobility with the available databases, the phase-field method is employed to investigate the microstructure evolutions in the $\gamma + \gamma'/\gamma$ and $\gamma + \gamma'/\gamma + \gamma'$ diffusion couples in the Ni–Al–Cr alloys. The effect of the antiphase relation of the γ' ordered domain on the interdiffusion process is mainly studied. It is found that the interaction among ordered domains can remarkably affect the interdiffusion process. Due to the different frequencies for the two coarsening mechanisms to appear in the one- and the four-domain systems in the precipitation process in the two diffusion couples, both the γ' precipitate morphology and the composition gradient near the diffusion zone in the one-domain system are different from those in the four-domain system, which leads to the difference in diffusion velocity and volume fraction of the γ' precipitate.

References

[1] Thompson M S and Morral J E 1986 *Acta Metall.* **34** 2201
[2] Thompson M S and Morral J E 1986 *Acta Metall.* **34** 339
[3] Thompson M and Morral J E 1987 *Metall. Mater. Trans.* A **18** 1565
[4] Thompson M, Morral J E and Romig A 1990 *Metall. Mater. Trans.* A **21** 2679
[5] Hopfe W D and Morral J E 1994 *Acta Metall. Mater.* **42** 3887
[6] Engstrom A, Morral J E and Ågren J 1997 *Acta Mater.* **45** 1189
[7] Dayananda M A and Kim C 1979 *Metall. Mater. Trans.* A **10** 1333
[8] Dayananda M A 1989 *Mater. Sci.* B **12** 341
[9] Dayananda M A 1989 *Mater. Sci. Eng.* A **120-121** 351
[10] Dayananda M A and Sohn Y H 1996 *Scr. Mater.* **35** 683
[11] Tortorici P C and Dayananda M A 1999 *Mater. Sci. Eng.* A **261** 64
[12] Morral J E 2005 *Tsinghua Sci. & Techn.* **10** 704
[13] Wu K, Morral J E and Wang Y 2001 *Acta Mater.* **49** 3401
[14] Chen Q, Ma N, Wu K and Wang Y 2004 *Scr. Mater.* **50** 471
[15] Wu K, Chang Y A and Wang Y 2004 *Scr. Mater.* **50** 1145
[16] Wu K, Morral J E and Wang Y 2004 *Acta Mater.* **52** 1917
[17] Wang Y and Khachaturyan A 1994 *Scr. Metall. Mater.* **31** 1425
[18] Wang Y, Banerjee D, Su C C and Khachaturyan A G 1998 *Acta Mater.* **46** 2983
[19] Zhu J Z, Liu Z K, Vaithyanathan V and Chen L Q 2002 *Scr. Mater.* **46** 401
[20] Kitashima T, Wang J and Harada H 2006 *J. Jpn. I. Met.* **70** 682
[21] Engström A and Ågren J 1996 *Z. Metall.* **87** 92
[22] Hu S Y and Chen L Q 2001 *Acta Mater.* **49** 1879
[23] Chen L Q and Shen J 1998 *Comput. Phys. Commun.* **108** 147